Citation: Cell Death and Disease (2011) 2, e181; doi:10.1038/cddis.2011.62

www.nature.com/cddis

Chemosensitization by phenothiazines in human lung cancer cells: impaired resolution of γH2AX and increased oxidative stress elicit apoptosis associated with lysosomal expansion and intense vacuolation

D Zong*[,1], P Hååg[1], I Yakymovych[1], R Lewensohn[1] and K Viktorsson*[,1]

Chemotherapy resistance poses severe limitations on the efficacy of anti-cancer medications. Recently, the notion of using novel combinations of 'old' drugs for new indications has garnered significant interest. The potential of using phenothiazines as chemosensitizers has been suggested earlier but so far our understanding of their molecular targets remains scant. The current study was designed to better define phenothiazine-sensitive cellular processes in relation to chemosensitivity. We found that phenothiazines shared the ability to delay γH2AX resolution in DNA-damaged human lung cancer cells. Accordingly, cells co-treated with chemotherapy and phenothiazines underwent protracted cell-cycle arrest followed by checkpoint escape that led to abnormal mitoses, secondary arrest and/or a form of apoptosis associated with increased endogenous oxidative stress and intense vacuolation. We provide evidence implicating lysosomal dysfunction as a key component of cell death in phenothiazine co-treated cells, which also exhibited more typical hallmarks of apoptosis including the activation of both caspase-dependent and -independent pathways. Finally, we demonstrated that vacuolation in phenothiazine co-treated cells could be reduced by ROS scavengers or the vacuolar ATPase inhibitor bafilomycin, leading to increased cell viability. Our data highlight the potential benefit of using phenothiazines as chemosensitizers in tumors that acquire molecular alterations rendering them insensitive to caspase-mediated apoptosis.

Cell Death and Disease (2011) **2,** e181; doi:10.1038/cddis.2011.62; published online 21 July 2011
Subject Category: Experimental Medicine

Genomic DNA constitutes a major target of many commonly used chemotherapeutic agents, including bleomycin and cisplatin. These drugs generate a complex array of DNA lesions some of which, such as DNA double-strand breaks (DSB) and interstrand crosslinks (ICLs), are highly lethal to proliferating cells by blocking DNA replication and transcription. To combat these toxic damages, mammalian cells are armed with several partially overlapping DNA repair pathways.[1] DNA DSBs trigger the prompt phosphorylation of serine-139 on histone H2AX (γH2AX), which serves as platforms to concentrate DNA repair factors locally at the sites of damage and to activate checkpoint proteins that enforce cell-cycle arrest.[2,3] In addition, non-DSB lesions such as ICLs also provoke γH2AX, possibly because ICLs can be converted into DSBs either by enzymatic activities during DNA repair[4] or through collapse of the replication fork in S phase.[5] Dephosphorylation of γH2AX is thought to take place concurrent to or after DNA repair and is required for efficient checkpoint recovery.[6] As checkpoint arrest is intimately coupled to DNA repair, premature resumption of cell division in the face of unrepaired DNA damage may cause chromosome separation defects resulting in mitotic catastrophe and cell death.[7] Indeed, the inability to resolve γH2AX is significantly correlated with decreased cell survival.[8] Thus, modulation of γH2AX clearance by inhibition of DNA repair or through other means has the potential to enhance tumor killing by DNA-damaging drugs.

DNA damage induces several forms of cell death, including apoptosis, necrosis and autophagic cell death.[9] Which of these death modes are induced in a given model system is dependent on cell-intrinsic properties, as well as the strength and duration of the death-inducing stimulus. Moreover, cell death with mixed features is often observed and multiple modes of cell death may also be simultaneously induced by a single drug under certain conditions. In general, DNA damage-induced apoptosis requires the activation of caspases, initiated mainly through the permeabilization of mitochondria by pro-apoptotic Bcl-2 family members Bax and Bak,[10] and to a lesser extent through membrane-proximal signaling from death receptors.[10] In addition, lysosomal dysfunction and persistent autophagy have been implicated in apoptosis upstream of mitochondrial permeabilization.[11,12]

[1]Department of Oncology and Pathology, Karolinska Biomics Center, Karolinska Institutet, Stockholm, Sweden
*Corresponding authors: D Zong, Karolinska Biomics Center Z5:01, Karolinska Institutet, SE-17176 Stockholm, Sweden. Tel: +46 8 517 750 95; Fax: +46 8 517 71 0000; E-mail: dali.zong@ki.se or K Viktorsson, Tel: +46 8 517 701 77; Fax: +46 8 517 71 0000; E-mail: kristina.viktorsson@ki.se
Keywords: phenothiazine; γH2AX, checkpoint recovery, apoptosis, lysosomes, oxidative stress
Abbreviations: AO, acridine orange; ATPase, adenosine triphosphatase; CFSE, carboxyfluorescein diacetate N-succinimidyl ester; CNS, central nervous system; CPZ, chlorpromazine; DNA-PK, DSB, double-strand break; FPZ, fluphenazine; ICL, interstrand crosslink; LMP, lysosomal membrane permeabilization; NAC, N-acetylcysteine; NSCLC, non-small cell lung carcinoma; PARP, poly (ADP-ribose) polymerase; ROS, reactive oxygen species; TFP, trifluoperazine; TFPZ, triflupromazine
Received 07.4.11; revised 03.6.11; accepted 14.6.11; Edited by V De Laurenzi

Increased generation of reactive oxygen species (ROS) is frequently observed in cells exposed to DNA-damaging agents[13] and depending on the particular model system, ROS signaling has been shown to induce apoptosis, autophagy, necrosis or premature senescence.[14] The intricate interplay between various stress-response pathways and their relation to cell death has not been clearly defined.

Phenothiazines are a class of compounds endowed with dopamine receptor antagonistic activities in the central nervous system (CNS), and are commonly used as part of anti-psychotic medication.[15] These compounds are also cytostatic and/or cytotoxic in a variety of non-CNS cells.[16] Interestingly, phenothiazines such as trifluoperazine (TFP) and chlorpromazine (CPZ) also possess chemosensitizing properties, although the mechanism behind this remains to be clarified. Our previous work implicated phenothiazines as candidate DNA repair inhibitors.[17] In the current study, we found a novel link between impairment of γH2AX clearance and enhancement of chemosensitivity by phenothiazines. We show that persistence of chemotherapy-induced γH2AX in phenothiazine co-treated lung cancer cells resulted in prolonged cell-cycle arrest followed by checkpoint escape, abnormal mitosis and subsequent induction of secondary arrest and/or cell death. Chemical inhibitor studies indicated ROS and the lysosomal compartment as relevant mediators of phenothiazine-induced chemosensitization, while caspases were important but not indispensable for cell death in this setting. Our data highlight the potential benefit of using phenothiazines as chemosensitizers in tumors that acquire molecular alterations rendering them insensitive to caspase-mediated apoptosis.

Results

Phenothiazines potentiate DNA damage-induced killing of human lung cancer cells. The clonogenic capacity of human non-small cell lung carcinoma (NSCLC) U1810 and H23 cells following DNA-damaging treatment was determined by colony formation assay in the absence and presence of 10 μM TFP (Figure 1a). TFP significantly augmented the cytotoxicity of bleomycin in U1810 cells (Figure 1b). Application of the Bliss additivism model indicated supra-additive combination effects across the entire dose range of bleomycin (Figure 1c). At equimolar concentrations, the efficacy of TFP as bleomycin sensitizer was superior to that of the DNA repair inhibitor NU7026 (Figure 1b). TFP also markedly enhanced cisplatin cytotoxicity in U1810 cells (Figure 1d). Moreover, TFP sensitized H23 cells to bleomycin and cisplatin (Supplementary Figure 1a). In addition to TFP, two other phenothiazines fluphenazine (FPZ) and triflupromazine (TFPZ) also sensitized U1810 cells to cisplatin (Supplementary Figure S1b). These data confirm phenothiazines as effective sensitizers of DNA-damaging chemotherapy.

Phenothiazines impair the resolution of chemotherapy-induced γH2AX. Phosphorylated H2AX (γH2AX) is a useful surrogate marker for the detection of DNA DSBs[18] as well as certain types of non-DSB lesions.[5] Exposure of U1810 and H23 cells to bleomycin (7.5 and 5 μg/ml, 1 h, respectively) resulted in immediate and maximal induction of γH2AX (Figure 2a, $t=0$). The removal of bleomycin-induced γH2AX appeared to be biphasic with a fast phase within the first 4 h post-treatment and a slow phase thereafter. Importantly, TFP significantly impeded the resolution of bleomycin-induced γH2AX during the fast phase in both U1810 and H23 cells (Figures 2a). Impairment of γH2AX resolution by TFP was also evident in U1810 cells exposed to a pharmacologically relevant concentration (2.5 μg/ml) of bleomycin (Figure 2b). In addition, TFPZ delayed γH2AX resolution in bleomycin-treated U1810 cells (Figure 2c). Unlike bleomycin, cisplatin triggered a gradual accrual of γH2AX in a subset of U1810 cells that peaked at 6 h post-treatment and declined thereafter (Figure 2d). After 12 and 24 h, TFP-co-treated U1810 cells harbored significantly higher levels of γH2AX, indicating that TFP also delayed the resolution of cisplatin-induced γH2AX (Figure 2d). The DNA repair inhibitor NU7026 behaved differently from TFP; NU7026 reduced the magnitude of γH2AX induction and prevented its removal in bleomycin-treated U1810 and H23 cells (Figure 2a), but did not affect either the induction or removal of γH2AX in cisplatin-treated U1810 cells (Figure 2d). These data demonstrated that phenothiazines share the ability to perturb γH2AX dynamics.

Phenothiazines delay the recovery of cells from chemotherapy-induced cell-cycle arrest. Phosphorylation and dephosphorylation of H2AX have been implicated in the activation and de-activation of DNA damage-inducible cell-cycle checkpoints, respectively.[2,6] We therefore set out to examine if impairment of γH2AX resolution by TFP perturbs checkpoint arrest of U1810 cells exposed to bleomycin or cisplatin (Figure 3 and Supplementary Figure 2). Bleomycin treatment caused progressive accumulation of cells in G_2-M, with a peak at about 12 h post-treatment (Figure 3a). In the absence of TFP, recovery from bleomycin-induced G_2-M arrest occurred between 6 and 12 h post-treatment, as shown by increases in the percentage of cells in G_1. On the contrary, only a minority of TFP-co-treated cells progressed from G_2-M to G_1 after 18 h, suggesting that TFP co-treatment largely prevented the inactivation of bleomycin-induced G_2-M checkpoint (Figure 3a). Importantly, TFP also retarded the recovery of U1810 cells from cisplatin-induced S phase checkpoint (Figure 3b). In the absence of TFP, most S phase cells recovered between 18 and 24 h post-treatment, as indicated by their progression into G_2-M and then G_1. By contrast, significant progression of TFP-co-treated cells was first detected between 24 and 36 h (Figure 3b). Thus, delay of γH2AX resolution by TFP impaired the recovery of U1810 cells from two molecularly distinct cell-cycle checkpoints triggered by different DNA lesions that is DNA DSBs *versus* ICLs.

Phenothiazines allow checkpoint escape leading to mitotic defects, secondary cell-cycle arrest and increased apoptosis. To further analyze the impact of TFP on checkpoint recovery after DNA damage, U1810 cells were pulse-labeled with CFSE before drug treatment and chased for up to 96 h. Mock-treated cells divided continuously, as indicated by the progressive dissipation of

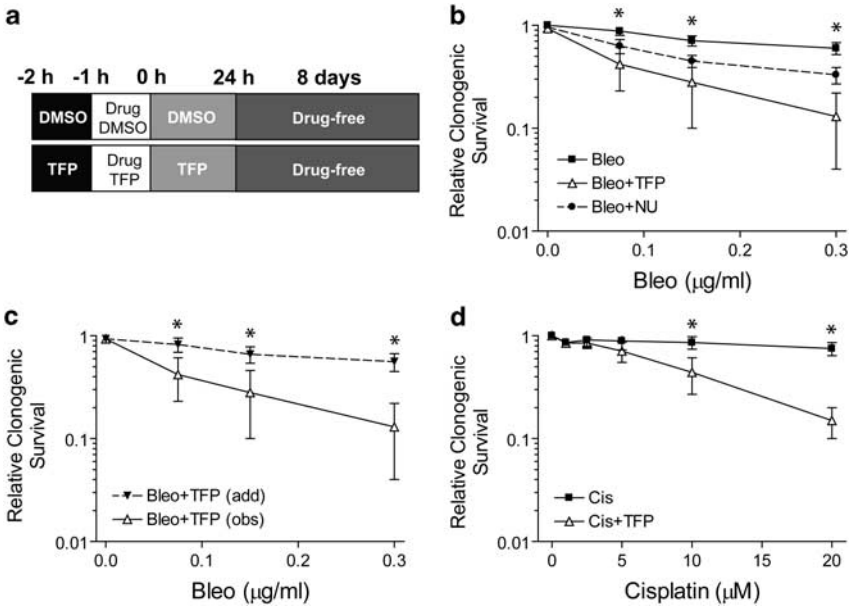

Figure 1 TFP potentiates DNA damage-induced killing of human lung cancer cells. Clonogenic capacity was determined for U1810 cells exposed to DNA-damaging drugs alone or in combination with TFP or NU7026 (both 10 μM). (**a**) Outline of drug co-treatment schemes: pre-treatment with 24 h post-incubation. For the sake of simplicity, only TFP co-treatment was shown, although the same strategy was also employed for other chemosensitizers. (**b**) TFP co-treatment markedly reduced the clonogenic capacity of cells exposed to bleomycin. (**c**) Comparison between the theoretical dose-response curve assuming additivity between bleomycin and TFP (*add*), as calculated from the Bliss additivism model, with the observed experimental data (*obs*) indicated that the combinatorial effect was supra-additive. (**d**) TFP significantly reduced the clonogenic capacity of cells exposed to cisplatin. Mean and S.D. were compiled from at least three independent experiments performed in duplicates (*$P<0.05$, TFP co-treatment *versus* single-agent bleo/cis treatment)

CFSE fluorescence (Figure 4a). By contrast, bleomycin-treated cells retained higher CFSE fluorescence initially after 24 h but the differences became insignificant over time (Figure 4a). This is consistent with a transient checkpoint-mediated cell-cycle arrest followed by recovery of proliferative capacity. In agreement with the slower resolution of γH2AX, TFP-co-treated cells initially exhibited even higher CFSE fluorescence than bleomycin-treated cells, indicating a more prolonged checkpoint response during the first 24 h post-treatment (Figure 4a). Importantly, although the majority of TFP-co-treated U1810 cells subsequently overcame the initial checkpoint arrest, the percentage of TFP-co-treated cells displaying hallmarks of abnormal mitosis increased significantly after 48 h (Figure 4b). A fraction of TFP-co-treated U1810 cells appeared to undergo secondary arrest 72 h post-treatment (Figure 4a, right panel). The emergence of this fraction, which was characterized by high CFSE fluorescence, was also evident when U1810 cells were co-treated with TFPZ (Figure 4a). Apoptotic DNA fragmentation was also abundant in TFP-co-treated cells as judged by nuclear morphology (Figure 4c) and hypo-diploid (subG$_1$) DNA content (data not shown). Furthermore, the above data clearly showed that abnormal mitosis preceded apoptosis. Conceivably, the escape of TFP-co-treated cells from DNA damage-induced checkpoints before complete resolution of γH2AX resulted in mitotic chromosomal separation defects that triggered apoptosis.

Phenothiazines augment the proteolytic cleavage and activation of multiple caspases after DNA-damaging treatment. Caspases are key mediators of apoptosis in response to a wide range of harmful insults, including DNA damage.[19] In agreement with its ability to enhance apoptosis based on morphological criteria, TFP also augmented caspase-3 activation in U1810 cells exposed to bleomycin or cisplatin (Figures 5a and b). The ability of TFP to augment caspase-3 activation was also observed in bleomycin-treated H23 cells and was shared by FPZ and CPZ (data not shown). Nuclear activity of caspase-3 was confirmed by the cleavage of its substrate PARP (Figure 5c). Notably, active caspase-3 was detected predominantly in U1810 cells with 4n DNA content (Figure 5a, right panel), suggesting that TFP may enhance apoptosis as a consequence of defective mitosis. Activation of caspase-3 can be mediated by multiple initiator caspases, including caspases-2, -8 and -9.[19] TFP significantly augmented the proteolytic cleavage of caspase-8 (Figure 5d and Supplementary Figure S3c) and caspase-9 (Figure 5e) in U1810 cells after DNA damage. The markedly increased level of catalytically active caspase-9 in TFP-co-treated U1810 cells (Figure 5f) was associated with conformational activation of Bak and Bax (Supplementary Figures S3a) and mitochondrial depolarization (Supplementary Figure S3b). Thus, TFP potentiated DNA damage-induced apoptosis by enhancing the activation of both the intrinsic and the extrinsic pathways.

Phenothiazine-mediated chemosensitization involves lysosomal dysfunction. Vacuolation is a phenomenon frequently observed in cells exposed to stressful stimuli, including chemotherapeutic drugs.[20] Bleomycin triggered vacuolation in U1810 cells that was visible by light

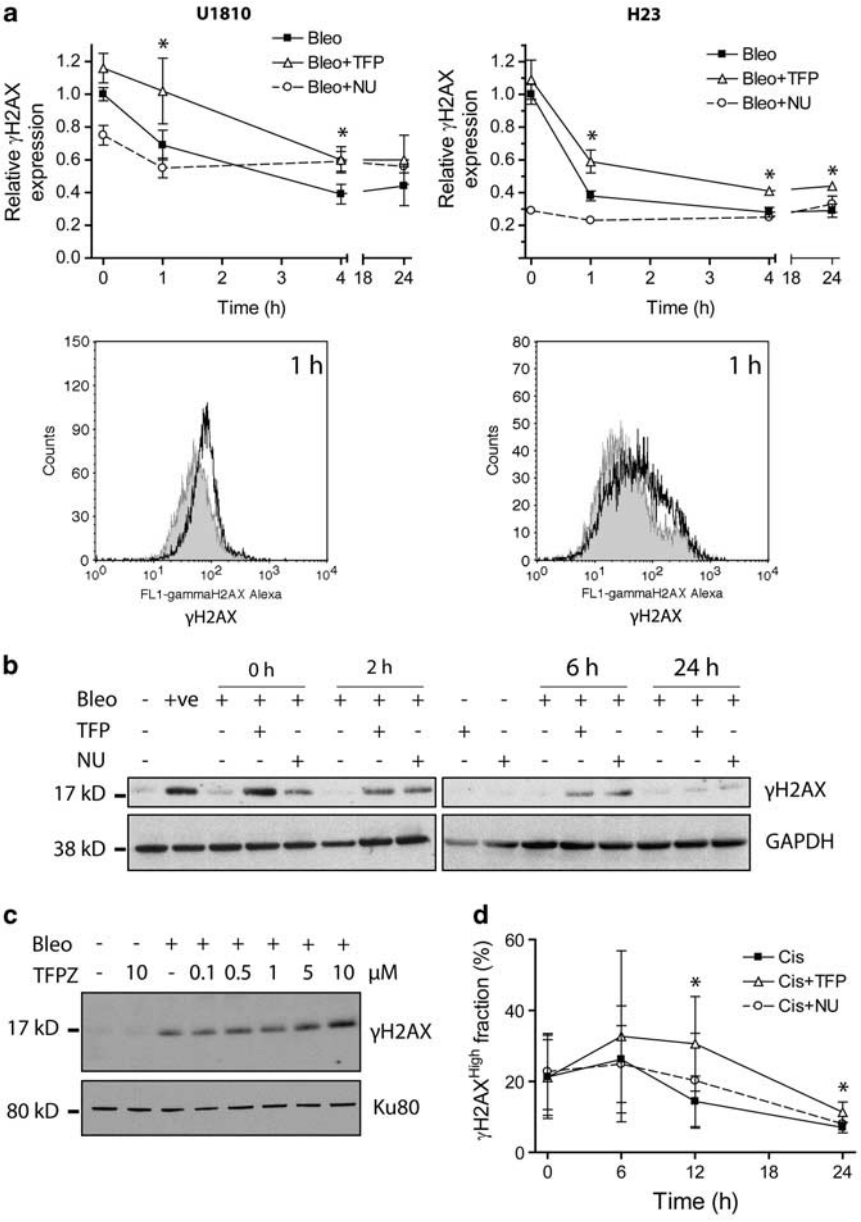

Figure 2 Phenothiazines delay γH2AX resolution in human lung cancer cells. Cells were exposed to DNA-damaging agents alone or in combination with TFP or NU7026 (both 10 μM). (**a**) TFP significantly delayed the resolution of γH2AX in U1810 and H23 cells exposed to 7.5 μg/ml bleomycin (top left) and 5 μg/ml bleomycin (top right), respectively. Phosphorylation of H2AX (Ser139) was quantified by flow cytometry using Alexa Fluor 488-conjugated antibodies. The histograms below highlight differences in cellular Alexa Fluor 488-associated fluorescence at 1 h post-bleomycin treatment: shaded, bleo; unshaded, bleo + TFP. For bleomycin-treated cells, the kinetics of γH2AX resolution is indicated by fold changes in the geometric mean of Alexa Fluor 488-associated fluorescence. An arbitrary value of 1 is assigned to samples collected immediately after bleomycin treatment in the absence of TFP ($t = 0$ h). (**b**) TFP retarded the resolution of γH2AX in U1810 cells exposed to 2.5 μg/ml bleomycin. Phosphorylated H2AX was detected by immunoblotting. (**c**) TFPZ impaired the resolution of γH2AX in U1810 cells 1 h after exposure to 15 μg/ml bleomycin. (**d**) TFP impeded the resolution of γH2AX in U1810 cells exposed to 50 μM cisplatin. As cisplatin induced γH2AX only in a subset of cells, the kinetics of γH2AX resolution in cisplatin-treated cells is defined by changes in the percentage of cells exhibiting high Alexa Fluor 488-associated fluorescence (γH2AX^{High} (%)). For (**a** and **d**), mean and S.D. were compiled from three independent experiments performed in duplicates (*$P < 0.05$, TFP co-treatment *versus* single-agent bleo/cis treatment). For (**b** and **c**), one representative experiment is shown ($n = 2$). + ve, positive control (20 μg/ml bleomycin, 1 h)

microscopy (Figure 6a) and manifested as time-dependent increases in side scattering during flow cytometric analysis (Figure 6b). This suggested that vacuolation constitutes a part of the cellular stress response to bleomycin in these cells. Strikingly, TFP-co-treated U1810 cells became intensely vacuolated over time (Figures 6a and b). Similar observations were also obtained for TFP-co-treated H23, H125 and U1752 cells (all NSCLC), and the ability of TFP to

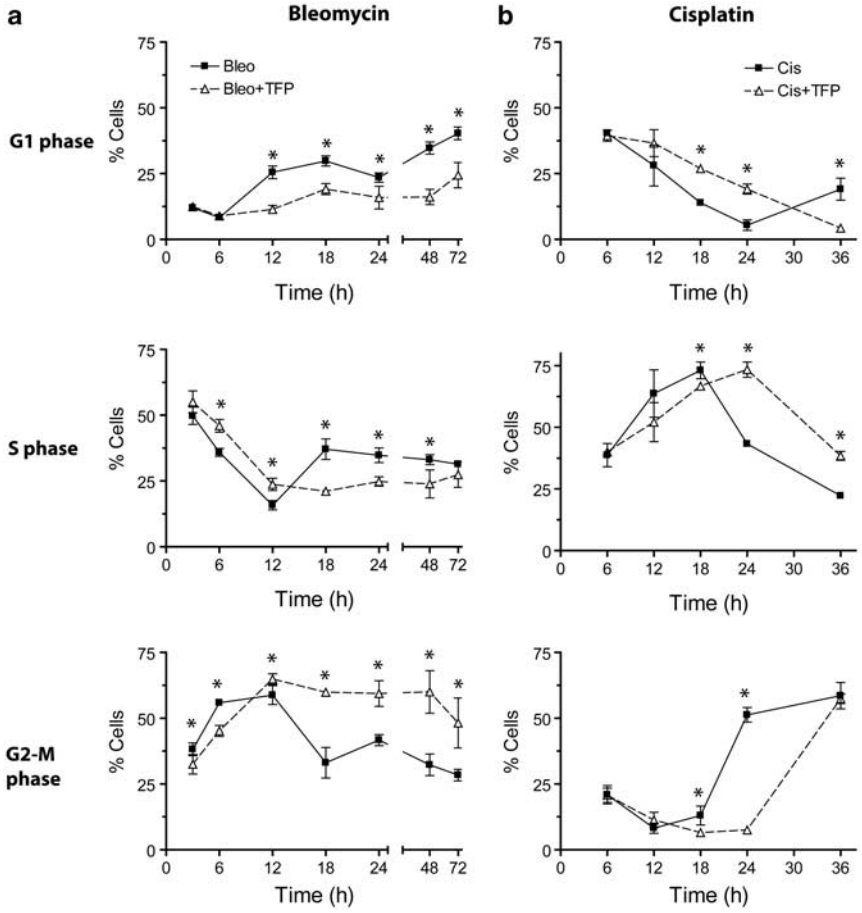

Figure 3 TFP delays the recovery of human lung cancer cells from DNA damage-induced checkpoints. U1810 cells were exposed to DNA-damaging drugs (2.5 μg/ml bleomycin, 20 μM cisplatin) alone or in combination with TFP (10 μM). At indicated time points, cell-cycle distribution was determined by DNA content analysis. The distribution of mock-treated cells and cells treated with TFP alone are omitted for the sake of simplicity, but can found in Supplementary Figure S2. (**a**) TFP significantly delayed the recovery of cells from bleomycin-induced G_2-M checkpoint arrest. (**b**) TFP significantly delayed the recovery of cells from cisplatin-induced intra-S checkpoint arrest. Mean and S.D. were compiled from at least three independent experiments performed in duplicates (*$P<0.05$, TFP co-treatment *versus* single-agent bleo/cis treatment)

enhance chemotherapy-induced vacuolation was shared by CPZ and FPZ (data not shown). A fraction of TFP-co-treated U1810 cells underwent lysosomal membrane permeabilization (LMP), as shown by decreased cellular retention of the acidophilic dye acridine orange (AO) (Figure 6c). On the whole population level, however, TFP-co-treated U1810 cells showed increased retention of AO over time (Figure 6d), suggesting that early LMP may lead to compensatory expansion of the cellular acidic compartment. We found an excellent correlation between AO retention and vacuolation (Figure 6e). In addition, TFP-co-treated U1810 cells stained more intensely with the lysosomotropic dye LysoTracker Green (Figure 6f), indicating that increased retention of AO by these cells may be due specifically to the expansion of lysosomal compartment causing vacuolation. Importantly, the vacuolar ATPase inhibitor bafilomycin A1 reduced the ability of TFP to enhance AO retention and caspase-3 activation in bleomycin-treated U1810 cells (Figures 6g and h). Similarly, bafilomycin A1 abrogated the potentiation of bleomycin-induced caspase-3 activation by CPZ, FPZ or TFPZ (data not shown). Taken together, these data suggested that phenothiazine-mediated chemosensitization involves lysosomal dysfunction upstream of caspase-3 activation.

Phenothiazine-mediated chemosensitization is associated with increased production of endogenous reactive oxygen species (ROS). Many classes of DNA-damaging agents are known to induce oxidative stress,[13,21,22] which is a major cause for dysfunction of cellular organelles and cell death.[14,23] Exposure of U1810 cells to bleomycin, cisplatin or TFP alone resulted in moderate increases of intracellular ROS (Figures 7a and b). Strikingly, TFP synergistically augmented cellular ROS production following treatment with bleomycin or cisplatin (Figures 7a and b). Interestingly, this TFP-mediated rise of intracellular ROS occurred much faster in bleomycin-treated cells than in cisplatin-treated cells, which is in agreement with the faster kinetics of apoptosis induction by bleomycin compared with cisplatin (Figure 4c). Regardless of the DNA-damaging agent, the onset of oxidative stress in TFP-co-treated U1810 cells (<24 h, Figures 7a and b) clearly preceded the activation of caspases (48 h, Figure 5). Importantly, the ROS scavenger N-acetylcysteine (NAC) mitigated oxidative stress and partially rescued the short-term viability as well as the long-term clonogenic capacity of TFP-co-treated U1810 cells (Figures 7c and d), suggesting that exacerbated oxidative stress contributes to the increased cytotoxicity of TFP co-treatment.

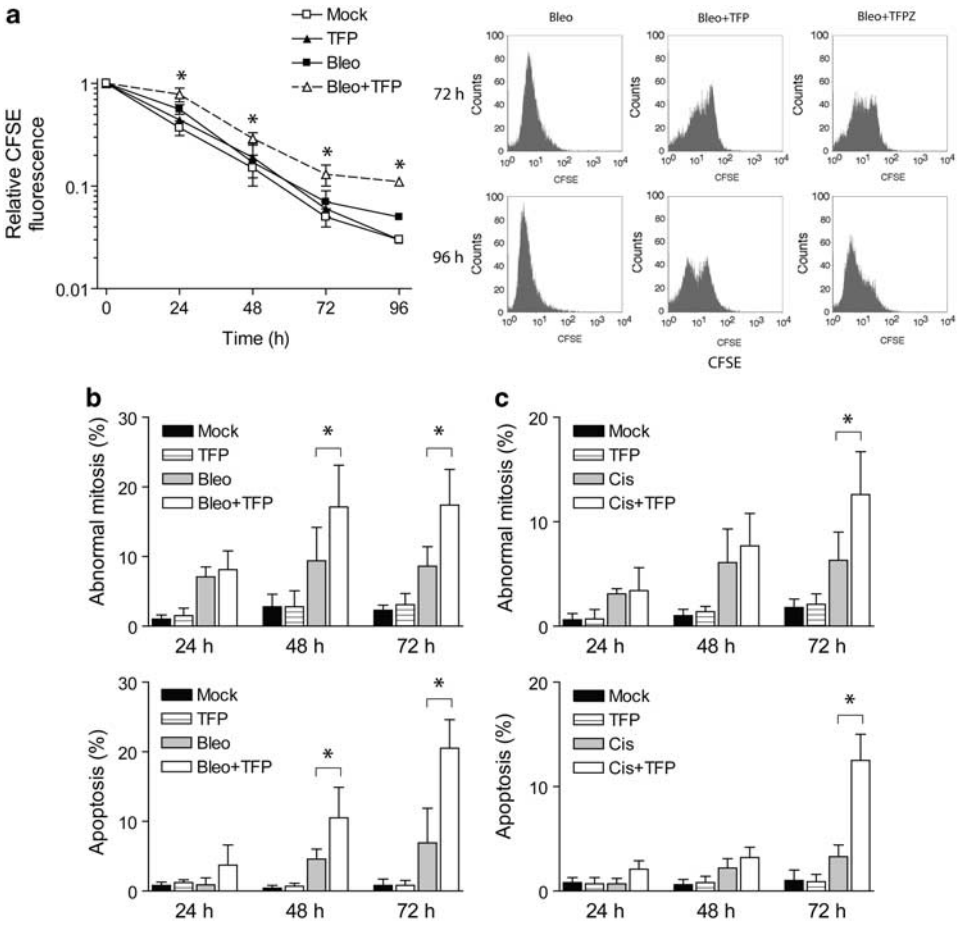

Figure 4 Phenothiazines promote secondary arrest and apoptosis in human lung cancer cells that recover from the initial DNA damage-induced checkpoints. U1810 cells were exposed to DNA-damaging drugs (2.5 μg/ml bleomycin, 20 μM cisplatin) alone or in combination with TFP (10 μM). (**a**) TFP markedly delayed the recovery of proliferative capacity of checkpoint-arrested U1810 cells (left); after 72 h, both TFP and TFPZ caused secondary arrest in a sub-population of cells (right). CFSE labeling was carried out 6 h before drug treatment. (**b**) TFP increased the percentage of bleomycin-treated cells that exhibit signs of abnormal mitosis (e.g., micronucleation, lagging chromosomes and anaphase bridges) and apoptosis (chromatin condensation and fragmentation, formation of apoptotic bodies). (**c**) TFP increased the percentage of cisplatin-treated cells that exhibit signs of abnormal mitosis and apoptosis. Mean and S.D. were compiled from three to four independent experiments performed in duplicates (*$P<0.05$, TFP co-treatment *versus* single-agent bleo/cis treatment)

Discussion

Phenothiazines are used routinely in the clinics as part of antipsychotic medication.[15] These compounds also possess well-documented chemosensitizing activities, although their mode(s) of action is unclear.[16,24] The current study was designed to map potential phenothiazine-sensitive cellular processes with relevance to chemosensitivity in lung cancer. In this study, we demonstrate for the first time the ability of phenothiazines to impede γH2AX resolution, which led to enhanced killing of human NSCLC cells by bleomycin and cisplatin. Phenothiazine-co-treated cells underwent prolonged initial checkpoint arrest followed by checkpoint escape, defective mitosis, dramatically increased ROS production and finally apoptosis associated with intense vacuolation and lysosomal expansion (Figure 8). Importantly, phenothiazine-mediated chemosensitization involves caspases but can also proceed via caspase-independent mechanisms. In light of the favorable toxicological profile of phenothiazines, our data support the notion that these compounds may be useful leads for the development of novel chemosensitizers against tumors that are insensitive to chemotherapy-induced caspase-mediated apoptosis.

We have previously identified TFP as a candidate DNA repair inhibitor.[17,25] However, we uncovered several notable differences between TFP and the DNA-PK kinase inhibitor NU7026. First, TFP was an efficient chemosensitizer of bleomycin and cisplatin, whereas NU7026 was only able to confer sensitization to bleomycin. Second, NU7026 but not TFP conferred radiosensitization in the tested NSCLC cell lines (data not shown), although we cannot rule out that this was due to certain cell-intrinsic defects. Third, the initial induction of γH2AX after bleomycin treatment was slightly enhanced by TFP but was markedly reduced by NU7026. These results indicated that TFP is probably not a direct kinase inhibitor of DNA-PK in intact cells. Nonetheless, TFP significantly retarded the resolution of γH2AX and recovery of proliferative capacity in U1810 and H23 cells after DNA-damaging treatment, suggesting that TFP somehow impaired the efficiency of DNA repair[17,26] and/or prevented the

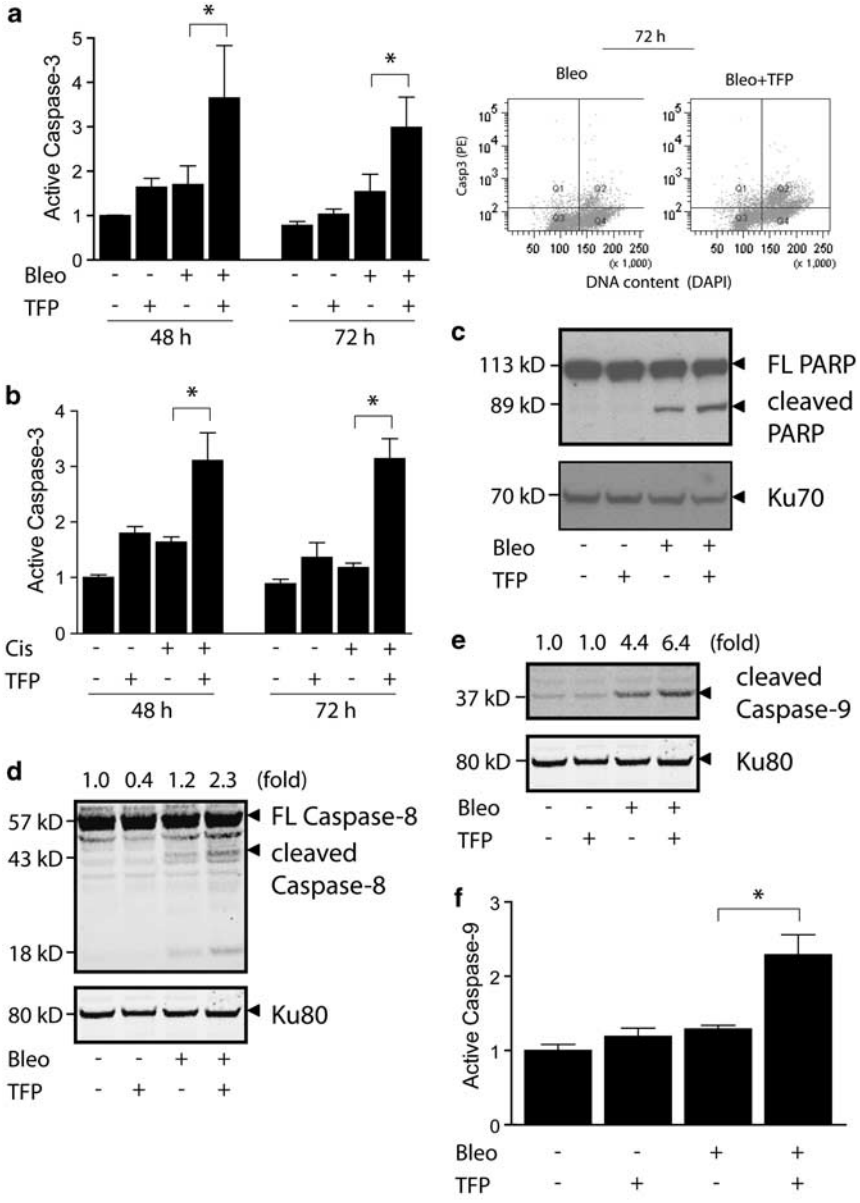

Figure 5 TFP augments the activation of both the extrinsic and the intrinsic apoptotic pathways after DNA damage. U1810 cells were exposed to DNA-damaging drugs (2.5 μg/ml bleomycin, 20 μM cisplatin) alone or in combination with TFP (10 μM). For immunoblotting and FLICA assay, samples were collected 48 h post DNA-damaging treatment. (**a**) TFP augmented caspase-3 activation after bleomycin treatment (left); enhanced caspase-3 activation was detected predominantly in cells containing 4n DNA content (right). (**b**) TFP potentiated caspase-3 activation after cisplatin treatment. (**c**) TFP co-treatment resulted in increased cleavage of PARP. (**d**) TFP co-treatment resulted in increased cleavage of caspase-8. (**e**) TFP co-treatment resulted in increased cleavage of caspase-9. (**f**) TFP-co-treated cells contain increased levels of catalytically active caspase-9. For (**a**, **b** and **f**), mean and S.D. were compiled from three independent experiments performed in duplicates (*$P<0.05$, TFP co-treatment *versus* single-agent bleo/cis treatment). For (**c**, **d** and **e**), the numbers at the top indicate the normalized intensity of the bands. One representative experiment is shown ($n=3$)

inactivation of signals that maintain cell-cycle checkpoints.[6] Importantly, the ability of TFP to retard γH2AX resolution was shared by TFPZ, suggesting that it may be a common property of phenothiazines. The accumulation of unresolved γH2AX in TFP-co-treated cells likely account for their decreased clonogenic capacity.[8]

A previous report showed that TFP enhanced G_2-M arrest in mouse leukemia cells exposed to bleomycin.[27] We show that TFP similarly enhanced the arrest of bleomycin-treated U1810 cells, which mostly accumulated in late G_2 and early mitosis, as judged by their positivity for phosphorylated (Ser10) histone H3 (data not shown), a marker for chromosome condensation.[28] There are two molecularly and temporally distinct G_2-M checkpoints: one of these is fast and enforces the arrest of cells that were in late S or early G_2 at the time they incur DNA damage, while the other is delayed and arrests cells that were in G_1 when they sustained DNA damage.[29] TFP appeared to prolong cell-cycle arrest mediated by both of these G_2-M checkpoints. In addition, TFP potentiated cisplatin-induced S-phase arrest in U1810

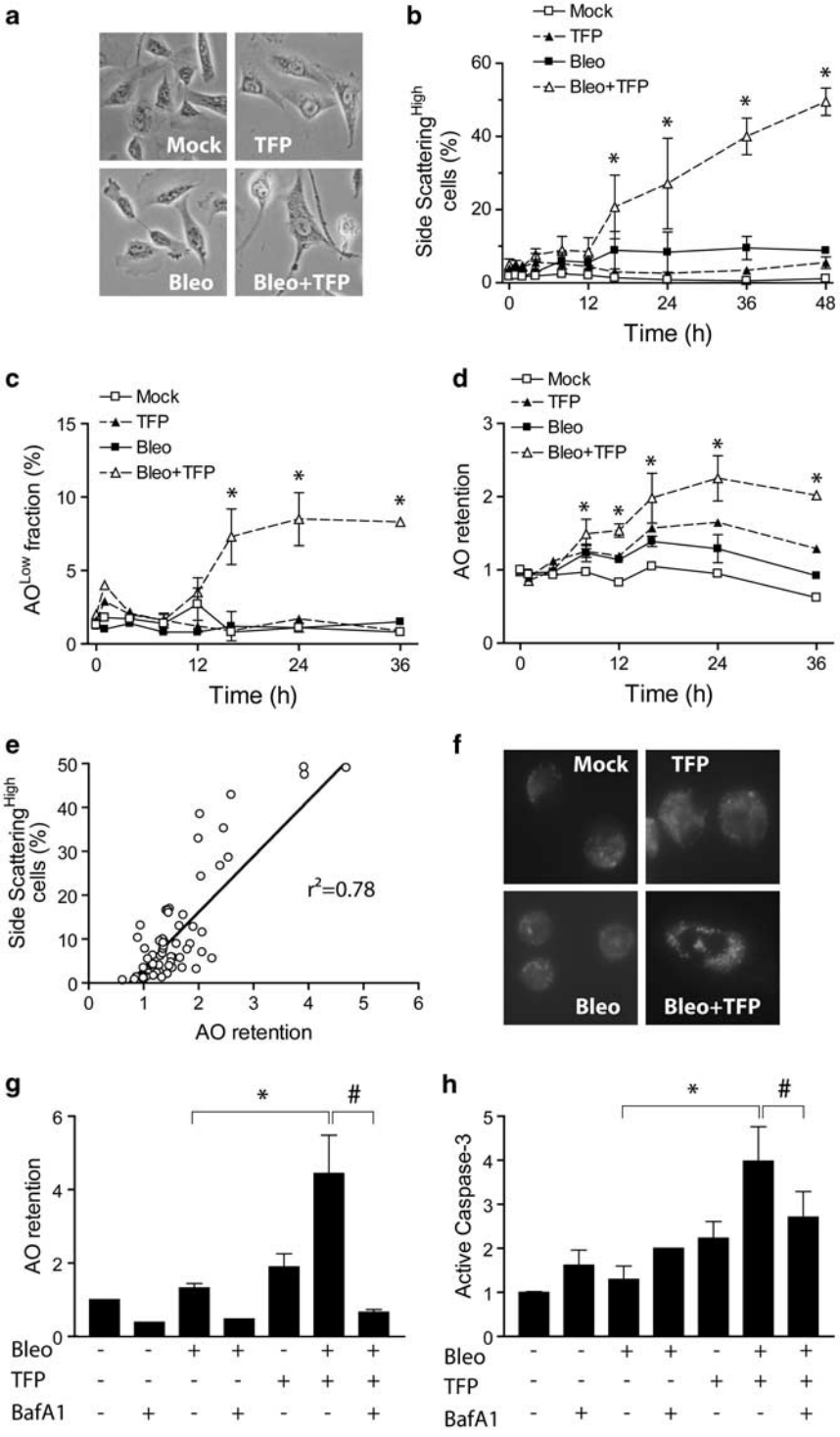

Figure 6 TFP causes lysosomal dysfunction and vacuolation after DNA damage. U1810 cells were exposed to bleomycin (2.5 μg/ml) alone or in combination with TFP (10 μM). (**a**) TFP co-treatment resulted in enlargement of cells and intense vacuolation after 48 h, as judged by light microscopy. (**b**) TFP-co-treated cells showed time-dependent increases in vacuolation, which manifested as increased side scattering during flow cytometric analysis. (**c**) TFP caused LMP, as indicated by decreased retention of AO, in a subset of bleomycin-treated cells. (**d**) TFP co-treatment induced dramatic expansion of intracellular acidic compartments, as judged by increased AO retention. (**e**) AO retention was positively correlated with vacuolation in U1810; data points cover the entire length of the experiments (0–48 h). (**f**) TFP co-treatment induced the expansion of lysosomal compartment, as judged by increased staining with LysoTracker Green. (**g**) Bafilomycin A1 reduced AO retention (after 48 h) in TFP-co-treated cells. (**h**) Bafilomycin A1 reduced caspase-3 activation (after 48 h) in TFP-co-treated cells. For (**g** and **h**), bafilomycin A1 (10 nM) was added 24 h post bleomycin treatment. Mean and S.D. were compiled from three to five independent experiments performed in duplicates ($^*P<0.05$, TFP co-treatment *versus* single-agent bleo treatment, $^{\#}P<0.05$, TFP co-treatment *versus* TFP co-treatment plus bafilomycin A1)

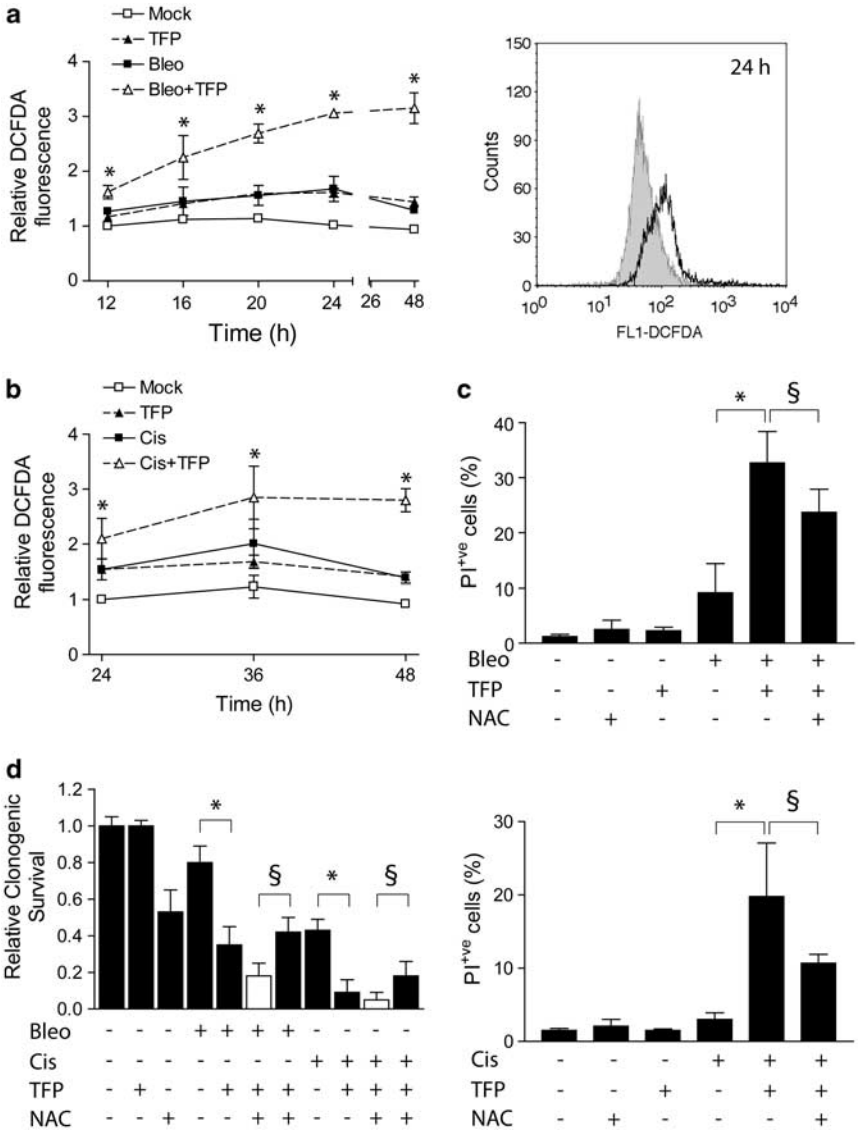

Figure 7 TFP increases endogenous ROS production after DNA-damaging treatment. U1810 cells were exposed to DNA-damaging drugs (2.5 μg/ml bleomycin, 20 μM cisplatin) alone or in combination with TFP (10 μM). Intracellular ROS was measured by oxidation of the probe CM-H_2DCFDA. Short-term cell viability was assayed by PI exclusion after 48 h (bleomycin) or 72 h (cisplatin); long-term clonogenic capacity was determined by standard colony formation assay after 9 days. (**a**) TFP-co-treated cells showed time-dependent increases in ROS production after exposure to bleomycin (left). The histogram (right) highlights differences in DCFDA-associated fluorescence after 24 h: shaded, bleo; unshaded, bleo + TFP. (**b**) TFP-co-treated cells showed time-dependent increases in ROS production after exposure to cisplatin. (**c**) N-acetylcysteine (NAC) partially rescued the short-term viability of cells co-treated with TFP and bleomycin (top) or cisplatin (bottom). NAC (10 mM, 48 h) was added immediately after bleomycin treatment and replenished once after 24 h. (**d**) NAC antagonized the suppression of long-term clonogenic capacity by TFP co-treatment. Filled columns, experimental data; open column, additive combinatorial effect as predicted by the Bliss model. Mean and S.D. were compiled from three to five independent experiments performed in duplicates (*$P < 0.05$, TFP co-treatment *versus* single-agent bleo/cis treatment, $^{\S}P < 0.05$, predicted additive combinatorial effects of TFP co-treatment plus NAC *versus* observed combinatorial effects of TFP co-treatment plus NAC)

cells, in accordance with the notion that cisplatin-induced replication stress triggers γH2AX.[5] It is worth pointing out that the S-phase checkpoint induced by cisplatin took longer time to activate compared with the G_2-M checkpoint induced by bleomycin, which was activated almost immediately. This helps explain why TFP impaired the resolution of bleomycin- and cisplatin-induced γH2AX with very different kinetics. More importantly, however, our data clearly showed that the ability of TFP to delay checkpoint recovery is not dependent on the type of checkpoint that was engaged.

A comparison of DNA content analysis with CFSE dilution dynamics revealed that phenothiazine delayed but did not prevent bleomycin-treated U1810 cells from escaping the initial G_2-M checkpoint, which occurred between 12 and 18 h post-treatment (as opposed to approximately 6 h post-treatment in the absence of phenothiazines). However, we observed a large increase in the number of cells bearing signs of defective mitoses and apoptosis, suggesting that the repair of bleomycin-induced DNA DSBs by phenothiazine co-treated cells was incomplete and/or imprecise. Enhanced

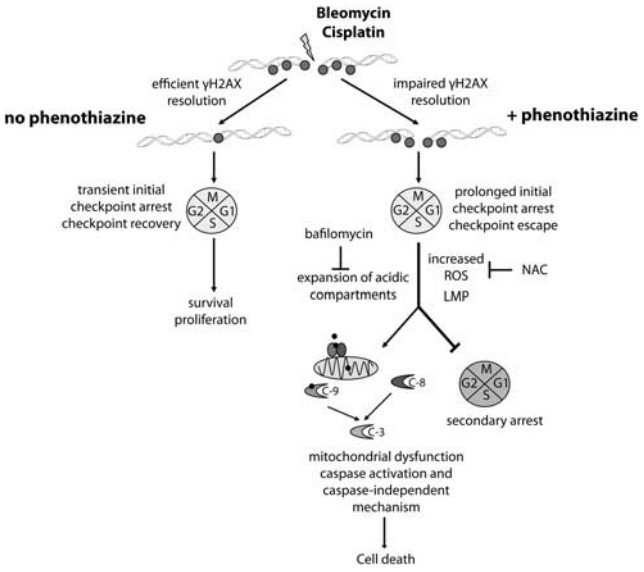

Figure 8 A working model for phenothiazine-mediated chemosensitization. Phenothiazines impair the resolution of γH2AX in human lung cancer cells that were exposed to DNA-damaging chemotherapy, causing prolonged checkpoint arrest followed by checkpoint escape, defective mitosis, secondary arrest and/or cell death. TFP co-treatment enhances the intracellular production of ROS, LMP and the subsequent uncontrolled expansion of acidic (lysosomal) compartments. The mode of cell death exhibits many molecular features associated with apoptosis, including chromatin fragmentation. Both caspase-dependent and caspase-independent mechanisms contribute to phenothiazine-mediated chemosensitization. C, caspase

caspase-3 activation has been reported as a feature of TFP-mediated chemosensitization in mouse cells,[27] although how it was achieved was not explored further. In this study we show for the first time that TFP and related phenothiazines augmented caspase-3 activation specifically in bleomycin-treated U1810 cells residing in G_2-M, possibly as a consequence of secondary arrest and/or aberrant mitosis. Moreover, we found that TFP enhanced the cleavage of both caspase-8 and caspase-9, indicating the activation of both the extrinsic and the intrinsic apoptotic pathways. Intriguingly, silencing of caspase-2 expression by siRNA partially reduced caspase-3 activation in TFP-co-treated U1810 cells (data not shown), although we could not detect caspase-2 cleavage by immunoblotting. In addition, increased mitochondrial depolarization and release of AIF (data not shown) were detected in TFP-co-treated cells. These data implicated the involvement of both caspase-dependent and caspase-independent pathways in phenothiazine-mediated chemosensitization, which explains the inability of z-VAD-fmk to rescue the clonogenic capacity of TFP-co-treated cells (data not shown).

We considered that phenothiazines may alter the permeability of plasma membrane,[30] which could influence drug uptake. Incubation of TFP for 2 h did not appreciably impact the ability of cells to exclude PI (data not shown), suggesting that increased drug influx through enhanced membrane permeability was unlikely. Phenothiazines are also lysosomotropic compounds with calmodulin antagonistic activities.[31,32] Notably, we found that phenothiazines induced intense vacuolation and increased retention of AO in bleomycin- or cisplatin-treated U1810 cells, both of which was reversed by bafilomycin A1. As TFP-co-treated cells also stained more intensely with LysoTracker Green, the increased retention of AO by these cells was most likely to due expansion of the lysosomal compartment. This phenomenon was not replicated by the calmodulin inhibitors calmidazolium or W7 in bleomycin-treated U1810 cells (data not shown), which argues against a key role for calmodulin antagonism in phenothiazine-mediated chemosensitization. Although some cell types may accumulate autophagic vacuoles before apoptosis,[12] vacuolation of TFP-co-treated U1810 cells did not involve lipidation of LC3 characteristic of classic autophagy[33] or increased expression of Bnip3,[34,35] a BH3-only protein that regulates autophagy capable of activating Bak and Bax (data not shown). In fact, the increased activation of Bak and Bax evident in TFP-co-treated cells could not be attributed to changes in the expression of Bim, Bid, Mcl-1, Bcl-X_L or Bcl-2 (data not shown). Interestingly, we observed LMP and marked oxidative stress in TFP-co-treated U1810 cells (12 h post-treatment) long before conformational activation of Bak and Bax was detected (40 h post-treatment). In this regard, LMP has been shown to generate ROS and induce cell death in a Bak/Bax-dependent fashion.[11,23] In turn, Bak/Bax-mediated mitochondrial permeabilization activates caspases, which further disturbs cellular bioenergetics[36] and exacerbates oxidative stress, finally leading to mitochondrial depolarization, permeability transition and release of AIF. Phenothiazines may weaken lysosomes by altering the fluidity of their lipid membrane,[30] making them more likely to rupture. Indeed, LMP was observed exclusively in TFP-co-treated cells. It is possible that ROS initially triggered vacuolation as a cyto-protective response to compensate for the loss of lysosomal functions through LMP.[20] However, the combination of LMP, ROS and mitochondrial dysfunction may be lethal to TFP-co-treated U1810 cells by creating a self-sustaining loop that leads to persistent oxidative stress and excessive vacuolation. In support of this notion, bafilomycin A1 suppressed the expansion of intracellular acidic compartment and abolished caspase-3 activation in phenothiazine co-treated cells. Moreover, the clonogenic capacity of TFP-co-treated cells could be partially restored by the anti-oxidant compound NAC, which reduced the ROS load in these cells. Taken together, these data identify ROS as a potentially important determinant of lysosomal integrity and an effector of phenothiazine-mediated chemosensitization. Our results highlight the need for further studies in which the clinical utility of phenothiazines as sensitizers of conventional chemotherapy is assessed especially in tumors refractory to chemotherapy-induced apoptosis.

Materials and Methods

Cells lines and culture conditions. Human NSCLC cell lines U1810 and H23 were used in the current study. U1810 was established from a patient tumor at the University of Uppsala, Sweden;[37] H23 was acquired from commercial sources (American Type Culture Collection, Manassas, VA, USA). Cells were cultured in RPMI-1640 medium containing L-glutamine and further supplemented with 10% heat-inactivated fetal calf serum, 100 IE/ml penicillin and 100 μg/ml streptomycin.

Drugs and drug co-treatment schemes. Bleomycin (Baxter Medical AB, Kista, Sweden) was dissolved in sterilized PBS. Cisplatin (Hospira Nordic AB, Stockholm, Sweden) was obtained in the form of ready-to-use infusion solution. Trifluoperazine dihydrochloride (TFP), fluphenazine dihydrochloride (FPZ),

chlorpromazine hydrochloride (CPZ) and triflupromazine hydrochloride (TFPZ, all from Sigma-Aldrich, Stockholm, Sweden) and the ATP-competitive DNA-PK inhibitor 2-(morpholin-4-yl)-benzo[h]chomen-4-one (NU7026, Calbiochem, Nottingham, UK) were prepared in DMSO and used at a final concentration of 10 μM. Drug co-treatment was carried out as follows (Figure 1a): exponentially growing cells were pre-treated with a chemosensitizer (1 h), then exposed to a DNA-damaging agent in the presence of the chemosensitizer (1 h), followed by post-incubation in medium containing the chemosensitizer (up to 24 h). Further post-incubation beyond 24 h was carried out in medium devoid of chemosensitizer. Cells that were treated with DNA-damaging agent alone received solvent (0.1% DMSO) instead of chemosensitizer.

Chemicals. Giemsa stain, acridine orange (AO), 4′,6-diamidino-2-phenylindole (DAPI), carboxyfluorescein diacetate N-succinimidyl ester (CFSE), N-acetylcysteine (NAC), calmidazolium chloride (CMZ), N-(6-Aminohexyl)-5-chloro-1-naphthalene-sulfonamide hydrochloride (W7) and bafilomycin A1 were from Sigma-Aldrich. Benzyloxycarbonyl-Val-Ala-Asp fluoromethylketone (z-VAD-fmk) was from BD PharMingen (San Jose, CA, USA). Propidium iodide (PI), tetramethylrhodamine ethyl ester perchlorate (TMRE), 5-(and-6)-chloromethyl-2′,7′-dichlorodihydro-fluorescein diacetate acetyl ester (CM-H_2DCFDA) and LysoTracker Green DND-26 were from Invitrogen (Stockholm, Sweden).

Colony formation assays. Homogeneous single-cell suspensions of U1810 and H23 cells were plated in 60 mm cell$^+$ culture dishes (Sarstedt, Landskrona, Sweden). TFP was given either as pre-treatment without post-incubation or pre-treatment with 24 h post-incubation. After 9–14 days, cells were fixed and stained with Giemsa and colonies consisting of more than 50 cells were counted under a light microscope. Relative clonogenic survival was calculated by normalizing surviving fractions against the plating efficiency of untreated cells. The Bliss additivism model was applied to define the combinatorial effect of bleomycin and TFP. The model is expressed by the equation $C = A + B–A*B$, where C is the expected combinatorial effect assuming bleomycin and TFP interact additively, while A and B are the *de facto* observed individual effect of bleomycin and TFP, respectively. A theoretical additive dose-response curve (add) was plotted and compared with the observed experimental data (obs). If the experimental curve is below the theoretical curve, the interaction is deemed supra-additive.

Flow cytometric analysis of cellular signaling events. Catalytically active caspase-9 was detected using the FLICA Caspase 9 detection kit (Immunochemistry Technologies LLC, Bloomington, MN, USA) as per manufacturer's instructions. Intracellular ROS and mitochondrial transmembrane potential were determined by the oxidation of the ROS indicator CM-H_2DCFDA (10 μM, 1 h) and retention of the potentiometric dye TMRE (50 nM, 30 min), respectively. The intracellular acidic compartment was stained with the acidophilic dye AO (5 μg/ml, 15 min). These fluorescent probe-based analyses were performed in non-fixed cells. Antibody-based analyses were performed on paraformaldehyde-fixed cells suspended in permeabilization buffer (0.1% Triton X-100 and 1% BSA in PBS). Phosphorylation of H2AX and activation of caspase-3 were assayed with Alexa Flour 488-conjugated anti-phospho-H2AX (2F3, BioLegend, San Diego, CA, USA) and phycoethryrin (PE)-conjugated anti-active caspase-3 (BD PharMingen) antibodies, respectively. Caspase-3 activation in relation to cellcycle positions was determined by two-color flow cytometry using DAPI as the DNA-labeling agent. Active Bak and Bax were probed with conformation-sensitive antibodies as described previously.[38] At least 10 000 events were recorded on Becton–Dickinson FACSCalibur or LSR II flow cytometers (BD Biosciences, San Jose, CA, USA) Data analysis was conducted using the built-in Cell Quest software.

Determination of cell-cycle profile, proliferative capacity and cell viability after DNA damage. Cells were fixed in 70% ethanol and analysis of DNA content by PI staining was performed as described by Darzynkiewicz and Huang.[39] cell–cycle distribution was assigned using ModFit LT (Verity Software House, Topsham, ME, USA). Recovery of proliferative capacity after DNA damage-induced G_2-M arrest was assessed by the CFSE labeling method. Briefly, U1810 cells were pulse-labeled with 2.5 μM CFSE for 5 min at room temperature, washed free of unincorporated dye and incubated in fresh medium. Drug treatment commenced 6 h after the completion of labeling and progressive dilution of CFSE fluorescence indicates cell proliferation. Cell viability was estimated by PI (1 μg/ml) exclusion. At least 10 000 events were collected. Only non-fixed cells were used for CFSE and PI exclusion assays.

Analysis of nuclear morphology. Cells were fixed in 4% formaldehyde, dropped onto slides, mounted with VectaShield containing DAPI (Immunkemi F&D AB, Järfälla, Sweden) and examined under a Zeiss Axioplan-2 fluorescence microscope at $\times$40magnification (Carl Zeiss Inc., Thornwood, NY, USA). Each sample was analyzed by counting 200 cells in randoml -selected visual fields. Nuclei displaying chromatin condensation and DNA fragmentation were scored as apoptotic. Actual mitotic defects (e.g., lagging chromosomes and anaphase bridges) as well as micronucleation in interphase cells (which arises as a consequence of defective mitosis) were collectively categorized as abnormal mitosis.

Immunoblotting. To obtain total cell lysate, cells were lysed in RIPA buffer (50 mM Tris-HCl, pH 7.4, 150 mM NaCl, 1 mM EDTA, 0.1% Na-deoxycholate and 1% NP-40) supplemented with protease and phosphatase inhibitor cocktail tablets (Roche Diagnostics AB, Stockholm, Sweden). Cytosolic fraction was obtained as described previously.[40] In all, 20–30 μg of lysates were resolved by SDS-PAGE (NuPAGE, Invitrogen). Immunoblotting was performed with primary antibodies recognizing caspase-8 (1C12), cleaved caspase-9 (Asp330), caspase-9, Bim, Bcl-X_L, Mcl-1, p38 (phospho-Thr183/Tyr185, all from Cell Signaling Technology, Danvers, MA, USA); Bid, Bnip3 (both from Abcam, Cambridge, UK); PARP (C2-10), caspase-2 (both from BD Transduction Laboratories, San Jose, CA, USA); apoptosis-inducing factor (AIF), Bcl-2 (both from Santa Cruz Biotechnologies, CA, USA); p21 (Calbiochem); histone H3 (phospho-Ser10, Millipore, Temecula, CA, USA). Where indicated, antibodies against Ku70, Ku80 (both from Abcam) or GAPDH (Trevigen, Gaithersburg, MD, USA) were used to control for equal loading. Horseradish peroxidase-linked secondary antibodies (GE Healthcare, Piscataway, NJ, USA) were used to visualize bands by enhanced chemiluminescence (Thermo Fisher Scientific, Waltham, MA, USA). Alternatively, IR-Dye-linked secondary antibodies (LI-COR Biosciences, Bad Homburg, Germany) were used to image bands on the Odyssey platform.

Statistical analysis. Unless otherwise stated, all experiments were performed in duplicates, and repeated three times. Data points are expressed as the mean $\pm$ S.D. Two-tailed unpaired Student's *t*-test was used to compare TFP co-treatment with single-agent DNA-damaging treatment. Asterisks (*) indicate statistical significance when $P<0.05$.

Conflict of Interest

The authors declare no conflict of interest.

Acknowledgements. This research was supported by grants from the Swedish Cancer Society, the Stockholm Cancer Society, the Stockholm County Council, the Swedish Research Foundation and the European Union (EC FP-6 Chemores and FP-7 Apo-Sys). We thank Mrs Birgitta Mörk for excellent technical assistance.

1. Sancar A, Lindsey-Boltz LA, Unsal-Kacmaz K, Linn S. Molecular mechanisms of mammalian DNA repair and the DNA damage checkpoints. *Annu Rev Biochem* 2004; **73**: 39–85.
2. Fernandez-Capetillo O, Chen HT, Celeste A, Ward I, Romanienko PJ, Morales JC *et al.* DNA damage-induced G2-M checkpoint activation by histone H2AX and 53BP1. *Nat Cell Biol* 2002; **4**: 993–997.
3. Paull TT, Rogakou EP, Yamazaki V, Kirchgessner CU, Gellert M, Bonner WM. A critical role for histone H2AX in recruitment of repair factors to nuclear foci after DNA damage. *Curr Biol* 2000; **10**: 886–895.
4. Hanada K, Budzowska M, Modesti M, Maas A, Wyman C, Essers J *et al.* The structure-specific endonuclease Mus81-Eme1 promotes conversion of interstrand DNA crosslinks into double-strands breaks. *Embo J* 2006; **25**: 4921–4932.
5. Olive PL, Banath JP. Kinetics of H2AX phosphorylation after exposure to cisplatin. *Cytometry B Clin Cytom* 2009; **76**: 79–90.
6. Bartek J, Lukas J. DNA damage checkpoints: from initiation to recovery or adaptation. *Curr Opin Cell Biol* 2007; **19**: 238–245.
7. Vakifahmetoglu H, Olsson M, Zhivotovsky B. Death through a tragedy: mitotic catastrophe. *Cell Death Differ* 2008; **15**: 1153–1162.
8. Banath JP, Klokov D, MacPhail SH, Banuelos CA, Olive PL. Residual gammaH2AX foci as an indication of lethal DNA lesions. *BMC Cancer* 2010; **10**: 4.
9. Edinger AL, Thompson CB. Death by design: apoptosis, necrosis and autophagy. *Curr Opin Cell Biol* 2004; **16**: 663–669.
10. Roos WP, Kaina B. DNA damage-induced cell death by apoptosis. *Trends Mol Med* 2006; **12**: 440–450.

11. Boya P, Andreau K, Poncet D, Zamzami N, Perfettini JL, Metivier D *et al.* Lysosomal membrane permeabilization induces cell death in a mitochondrion-dependent fashion. *J Exp Med* 2003; **197**: 1323–1334.
12. Gonzalez-Polo RA, Boya P, Pauleau AL, Jalil A, Larochette N, Souquere S *et al.* The apoptosis/autophagy paradox: autophagic vacuolization before apoptotic death. *J Cell Sci* 2005; **118**: 3091–3102.
13. Pham NA, Hedley DW. Respiratory chain-generated oxidative stress following treatment of leukemic blasts with DNA-damaging agents. *Exp Cell Res* 2001; **264**: 345–352.
14. Ozben T. Oxidative stress and apoptosis: impact on cancer therapy. *J Pharm Sci* 2007; **96**: 2181–2196.
15. Shen WW. A history of antipsychotic drug development. *Compr Psychiatry* 1999; **40**: 407–414.
16. Motohashi N, Kawase M, Satoh K, Sakagami H. Cytotoxic potential of phenothiazines. *Curr Drug Targets* 2006; **7**: 1055–1066.
17. Polischouk AG, Holgersson A, Zong D, Stenerlow B, Karlsson HL, Moller L *et al.* The antipsychotic drug trifluoperazine inhibits DNA repair and sensitizes non small cell lung carcinoma cells to DNA double-strand break induced cell death. *Mol Cancer Ther* 2007; **6**: 2303–2309.
18. Sedelnikova OA, Rogakou EP, Panyutin IG, Bonner WM. Quantitative detection of (125)IdU-induced DNA double-strand breaks with gamma-H2AX antibody. *Radiat Res* 2002; **158**: 486–492.
19. Kumar S. Caspase function in programmed cell death. *Cell Death Differ* 2007; **14**: 32–43.
20. Henics T, Wheatley DN. Cytoplasmic vacuolation, adaptation and cell death: a view on new perspectives and features. *Biol Cell* 1999; **91**: 485–498.
21. Jing XB, Cai XB, Hu H, Chen SZ, Chen BM, Cai JY. Reactive oxygen species and mitochondrial membrane potential are modulated during CDDP-induced apoptosis in EC-109 cells. *Biochem Cell Biol* 2007; **85**: 265–271.
22. Wallach-Dayan SB, Izbicki G, Cohen PY, Gerstl-Golan R, Fine A, Breuer R. Bleomycin initiates apoptosis of lung epithelial cells by ROS but not by Fas/FasL pathway. *Am J Physiol Lung Cell Mol Physiol* 2006; **290**: L790–L796.
23. Zhao M, Eaton JW, Brunk UT. Bcl-2 phosphorylation is required for inhibition of oxidative stress-induced lysosomal leak and ensuing apoptosis. *FEBS Lett* 2001; **509**: 405–412.
24. Sudeshna G, Parimal K. Multiple non-psychiatric effects of phenothiazines: a review. *Eur J Pharmacol* 2010; **648**: 6–14.
25. Eriksson A, Yachnin J, Lewensohn R, Nilsson A. DNA-dependent protein kinase is inhibited by trifluoperazine. *Biochem Biophys Res Commun* 2001; **283**: 726–731.
26. Gangopadhyay S, Karmakar P, Dasgupta U, Chakraborty A. Trifluoperazine stimulates ionizing radiation induced cell killing through inhibition of DNA repair. *Mutat Res* 2007; **633**: 117–125.
27. Sullivan GF, Garcia-Welch A, White E, Lutzker S, Hait WN. Augmentation of apoptosis by the combination of bleomycin with trifluoperazine in the presence of mutant p53. *J Exp Ther Oncol* 2002; **2**: 19–26.
28. Hendzel MJ, Wei Y, Mancini MA, Van Hooser A, Ranalli T, Brinkley BR *et al.* Mitosis-specific phosphorylation of histone H3 initiates primarily within pericentromeric heterochromatin during G2 and spreads in an ordered fashion coincident with mitotic chromosome condensation. *Chromosoma* 1997; **106**: 348–360.
29. Xu B, Kim ST, Lim DS, Kastan MB. Two molecularly distinct G(2)/M checkpoints are induced by ionizing irradiation. *Mol Cell Biol* 2002; **22**: 1049–1059.
30. Michalak K, Wesolowska O, Motohashi N, Molnar J, Hendrich AB. Interactions of phenothiazines with lipid bilayer and their role in multidrug resistance reversal. *Curr Drug Targets* 2006; **7**: 1095–1105.
31. Daniel WA. Mechanisms of cellular distribution of psychotropic drugs. Significance for drug action and interactions. *Prog Neuropsychopharmacol Biol Psychiatry* 2003; **27**: 65–73.
32. Hait WN, Lazo JS. Calmodulin: a potential target for cancer chemotherapeutic agents. *J Clin Oncol* 1986; **4**: 994–1012.
33. Kabeya Y, Mizushima N, Ueno T, Yamamoto A, Kirisako T, Noda T *et al.* LC3, a mammalian homologue of yeast Apg8p, is localized in autophagosome membranes after processing. *Embo J* 2000; **19**: 5720–5728.
34. Kubli DA, Ycaza JE, Gustafsson AB. Bnip3 mediates mitochondrial dysfunction and cell death through Bax and Bak. *Biochem J* 2007; **405**: 407–415.
35. Zeng X, Kinsella TJ. BNIP3 is essential for mediating 6-thioguanine- and 5-fluorouracil-induced autophagy following DNA mismatch repair processing. *Cell Res* 2010; **20**: 665–675.
36. Ricci JE, Munoz-Pinedo C, Fitzgerald P, Bailly-Maitre B, Perkins GA, Yadava N *et al.* Disruption of mitochondrial function during apoptosis is mediated by caspase cleavage of the p75 subunit of complex I of the electron transport chain. *Cell* 2004; **117**: 773–786.
37. Bergh J, Nilsson K, Ekman R, Giovanella B. Establishment and characterization of cell lines from human small cell and large cell carcinomas of the lung. *Acta Pathol Microbiol Immunol Scand A* 1985; **93**: 133–147.
38. Mandic A, Viktorsson K, Molin M, Akusjarvi G, Eguchi H, Hayashi SI *et al.* Cisplatin induces the proapoptotic conformation of Bak in a deltaMEKK1-dependent manner. *Mol Cell Biol* 2001; **21**: 3684–3691.
39. Darzynkiewicz Z, Huang X. Analysis of cellular DNA content by flow cytometry. *Curr Protoc Immunol Chapter* 2004; **5**: Unit 5 7.
40. Shen J, Vakifahmetoglu H, Stridh H, Zhivotovsky B, Wiman KG. PRIMA-1MET induces mitochondrial apoptosis through activation of caspase-2. *Oncogene* 2008; **27**: 6571–6580.

Supplementary Information accompanies the paper on Cell Death and Disease website (http://www.nature.com/cddis)